



Universiteit
Leiden
The Netherlands

Spinocerebellar ataxia type 1 characteristics in patient-derived fibroblast and iPSC-derived neuronal cultures

Buijsen, R.A.M.; Hu, M.C.; Saez-Gonzalez, M.; Notopoulou, S.; Mina, E.; Koning, W.; ... ; Roon-Mom, W.M.C. van

Citation

Buijsen, R. A. M., Hu, M. C., Saez-Gonzalez, M., Notopoulou, S., Mina, E., Koning, W., ... Roon-Mom, W. M. C. van. (2023). Spinocerebellar ataxia type 1 characteristics in patient-derived fibroblast and iPSC-derived neuronal cultures. *Movement Disorders*, 38(8), 1428-1442. doi:10.1002/mds.29446

Version: Publisher's Version
License: [Creative Commons CC BY-NC-ND 4.0 license](https://creativecommons.org/licenses/by-nc-nd/4.0/)
Downloaded from: <https://hdl.handle.net/1887/3762277>

Note: To cite this publication please use the final published version (if applicable).

RESEARCH ARTICLE

Spinocerebellar Ataxia Type 1 Characteristics in Patient-Derived Fibroblast and iPSC-Derived Neuronal Cultures

Ronald A.M. Buijsen, PhD,^{1*} Michel Hu, MSc,^{1,2} Maria Sáez-González, MSc,¹ Sofia Notopoulou, MSc,³ Eleni Mina, PhD,¹ Winette Koning, MSc,¹ Sarah L. Gardiner, MD, PhD,^{1,2} Linda M. van der Graaf, BSc,¹ Elena Daoutsali, MSc,¹ Barry A. Pepers, BSc,¹ Hailiang Mei, PhD,⁴ Vera van Dis, PhD,^{5,6} Jean-Philippe Frimat, PhD,^{1,2} Arn M. J. M. van den Maagdenberg, PhD,^{1,2} Spyros Petrakis, PhD,³ and Willeke M.C. van Roon-Mom, PhD¹

¹Department of Human Genetics, Leiden University Medical Center, Leiden, Zuid-Holland, The Netherlands

²Department of Neurology, Leiden University Medical Center, Leiden, Zuid-Holland, The Netherlands

³Institute of Applied Biosciences, Centre for Research and Technology Hellas, Thessaloniki, Greece

⁴Department of Biomedical Data Sciences, Leiden University Medical Center, Leiden, Zuid-Holland, The Netherlands

⁵Department of Pathology, Leiden University Medical Center, Leiden, Zuid-Holland, The Netherlands

⁶Department of Pathology, Erasmus Medical Center, Rotterdam, Zuid-Holland, The Netherlands

ABSTRACT: Background: Spinocerebellar ataxia type 1 (SCA1) is a neurodegenerative disease caused by a polyglutamine expansion in the ataxin-1 protein resulting in neuropathology including mutant ataxin-1 protein aggregation, aberrant neurodevelopment, and mitochondrial dysfunction.

Objectives: Identify SCA1-relevant phenotypes in patient-specific fibroblasts and SCA1 induced pluripotent stem cells (iPSCs) neuronal cultures.

Methods: SCA1 iPSCs were generated and differentiated into neuronal cultures. Protein aggregation and neuronal morphology were evaluated using fluorescent microscopy. Mitochondrial respiration was measured using the Seahorse Analyzer. The multi-electrode array (MEA) was used to identify network activity. Finally, gene expression changes were studied using RNA-seq to identify disease-specific mechanisms.

Results: Bioenergetics deficits in patient-derived fibroblasts and SCA1 neuronal cultures showed altered oxygen consumption rate, suggesting involvement of mitochondrial dysfunction in SCA1. In SCA1 hiPSC-derived neuronal cells, nuclear and cytoplasmic

aggregates were identified similar in localization as aggregates in SCA1 postmortem brain tissue. SCA1 hiPSC-derived neuronal cells showed reduced dendrite length and number of branching points while MEA recordings identified delayed development in network activity in SCA1 hiPSC-derived neuronal cells. Transcriptome analysis identified 1050 differentially expressed genes in SCA1 hiPSC-derived neuronal cells associated with synapse organization and neuron projection guidance, where a subgroup of 151 genes was highly associated with SCA1 phenotypes and linked to SCA1 relevant signaling pathways.

Conclusions: Patient-derived cells recapitulate key pathological features of SCA1 pathogenesis providing a valuable tool for the identification of novel disease-specific processes. This model can be used for high throughput screenings to identify compounds, which may prevent or rescue neurodegeneration in this devastating disease. © 2023 The Authors. *Movement Disorders* published by Wiley Periodicals LLC on behalf of International Parkinson and Movement Disorder Society.

This is an open access article under the terms of the [Creative Commons Attribution-NonCommercial-NoDerivs](#) License, which permits use and distribution in any medium, provided the original work is properly cited, the use is non-commercial and no modifications or adaptations are made.

*Correspondence to: Dr. Ronald A.M. Buijsen, Department of Human Genetics Leiden University Medical Center, Einthovenweg 20, Leiden, Zuid-Holland, 2333 ZC, The Netherlands; E-mail: r.a.m.buijsen@lumc.nl

Relevant conflicts of interest/financial disclosures: The authors have no conflicts of interest to declare. All co-authors have seen and agree with the contents of the manuscript and there is no financial interest to report. We certify that the submission is original work and is not under review at any other publication.

Funding agencies: This research is funded by Hersenstichting (Dutch Brain Foundation) projects HA2016-02-02 (W.M.C.v.R.-M.), DR-2018-00253 (R.A.M.B.), and ZonMw PTO2 project 446002002 (R.A.M.B. and W.M.C.v.R.-M.). This work was supported by the Netherlands Organ-on-Chip Initiative, an NWO Gravitation project (024.003.001) funded by the Ministry of Education, Culture and Science of the government of the Netherlands (A.M.J.M.v.d.M. and J.P.F.).

Michel Hu, Maria Sáez-González, and Sofia Notopoulou are shared second authors.

Received: 12 January 2023; **Revised:** 23 March 2023; **Accepted:** 20 April 2023

Published online 6 June 2023 in Wiley Online Library (wileyonlinelibrary.com). DOI: 10.1002/mds.29446

Key Words: bioenergetics; disease modelling; electrophysiology; human induced pluripotent stem cells; MEA;

neurodegeneration; neuronal aggregates; neuronal morphology; RNA sequencing; spinocerebellar ataxia type 1

Introduction

Spinocerebellar ataxia type 1 (SCA1) is a neurodegenerative disorder characterized by progressive degeneration that is most severe in the cerebellum and brainstem.¹ The prevalence of SCA1 worldwide is 1 to 2 per 100,000 individuals^{2,3} with the main symptom being progressive cerebellar ataxia characterized by coordination and balance problems.⁴ Other signs include swallowing difficulties, oral musculature weakness, muscle stiffness, and extraocular muscles weakening leading to rapid, involuntary eye movements.⁴ Disease onset and duration are variable, but the disease typically manifests itself in the third or fourth decade of life and the average period from symptom onset to death varies from 10 to 30 years.⁵

SCA1 is an autosomal dominant disorder caused by a cytosine-adenine-guanine (CAG)-repeat expansion in exon 8 of the *ATXN1* gene.⁶ In healthy individuals, *ATXN1* alleles contain 6 to 35 CAG-repeats, whereas disease-causing alleles contain over 39 CAG-repeats.^{7,8} These CAG-repeats are translated into a polyglutamine (polyQ) tract in the ataxin-1 protein. There are eight other autosomal dominant neurodegenerative polyQ disorders, consisting of five other polyQ SCAs, Huntington's disease (HD), dentatorubral-pallidoluysian atrophy, and spinal and bulbar muscular atrophy.⁹⁻¹¹ Ataxin-1 is involved in several cellular processes including transcriptional regulation and RNA processing.^{11,12} SCA1 is caused by a proteotoxic-gain-of-function mechanism and polyQ expanded ataxin-1 forms aggregates in brain tissue of SCA1 patients.¹² These aggregates are reported as small (~1 to 2 μm), intranuclear aggregates and are present throughout the brain, both in affected and less affected brain areas.^{12,13} Aggregates are considered a pathological hallmark of polyQ disorders and correlate with disease progression in SCA1 animal models.^{14,15} Other main neuropathological findings are a marked loss of Purkinje neurons in the cerebellum and neurons of the dentate, basal pontine, and olivary nuclei, but as the disease progresses, other brain regions are also affected.¹²

Mutant ataxin-1 is involved in dysregulation of plasticity and synaptic function during cerebellar development.^{18,19} It changes the neural circuitry of the developing cerebellum in a SCA1-knockin mouse model and inhibits the formation and functionality of synaptic contacts of Purkinje neurons. This aberrant synaptogenesis leads to an excitatory/inhibitory imbalance causing cell damage and making SCA1 neurons more vulnerable later in life.¹⁶ In addition, conditional

SCA1 mice showed greatly diminished cerebellar pathology and motor phenotypes when mutant ataxin-1 expression is silenced until cerebellar development is completed,¹⁷ suggesting a neurodevelopmental role for ataxin-1.

Mitochondrial dysfunction and oxidative stress are implicated in SCA1 and other polyQ disorders.¹⁸⁻²² SCA1 mouse models demonstrate alterations in mitochondrial proteins, impairment of the electron transport chain (ETC) complexes, decrease in adenosine triphosphate (ATP) activity, and deficits in mitochondrial oxidative phosphorylation.²³⁻²⁵ These are important disease-modifying processes as both motor behavior deficits and disease pathology can be ameliorated in SCA1 mouse models by the mitochondria-targeting antioxidant MitoQ or the ETC complex II electron donor, succinic acid.^{25,27}

Despite advances in SCA1 research, there is no cure for SCA1.⁹ For the development of novel treatments, there is a need to establish patient-derived disease models that mimic main aspects of the disease. Human induced pluripotent stem cells (hiPSCs) derived from patients can be used for in vitro disease modeling.²⁶ These cell models have been used to study pathogenic processes, including protein aggregation, Purkinje cell (PC) development, and altered composition of glutamatergic receptors and test intervention strategies for polyQ diseases.^{20,27-31} We previously generated and characterized three hiPSC clones of a SCA1 patient, but so far, SCA1 hiPSC-based disease modeling has not been described.³²

Here, we describe additional skin fibroblasts totaling four SCA1 patients and four control individuals demonstrating defects in basal respiration and intracellular ATP levels in SCA1 cells. Next, we generated and characterized hiPSCs clones and observed ataxin-1 aggregates, defects in neuron process length and branching, altered neuronal network activity and mitochondrial dysfunction and in SCA1 hiPSC-derived neurons. Ataxin-1 positive aggregates were present in both the nucleus and cytoplasm of patient-derived neurons as was observed also in SCA1 post-mortem brain tissue. Last, we identified 1050 differentially expressed genes participating in processes related to neurodegeneration, regulating cellular metabolism, and signaling pathways in SCA1 hiPSC-derived neurons.

Collectively, SCA1 hiPSC-derived neuronal cultures recapitulate key pathological features of the disease providing a valuable tool for the investigation of pathogenic disease mechanisms and the identification of

compounds, which may prevent or rescue neurodegeneration in this devastating disease.

Methods

Standard Protocol Approval and Patient Consent

This study was approved by the Leiden University Medical Center (LUMC) medical ethics committee (NL45478.058.13/P13.080) and written informed consent was obtained from all participants. The age at onset was defined as the onset of motor impairment. Disease severity was assessed according to the scale for the assessment and rating of ataxia (SARA), the Stroop color and word test and the Mini-Mental State Examination.³³

Post-Mortem Brain Tissue

Post-mortem brain tissue was obtained from a male SCA1 patient, 52 years of age. Brain tissue was formalin fixed for about 3 months and embedded in paraffin. Samples were cut on a microtome (4 μ m) and evaluated using hematoxylin and eosin staining. Additional immunohistochemistry for ubiquitin (Table 1) was performed according to standard protocols and evaluated by a neuropathologist.

Generation and Characterization of hiPSCs

Generation and characterization of hiPSCs was performed as previously described.³³ HiPSCs from SCA1 patients and non-affected matched controls were generated using non-integrating Sendai viruses (SeV). These hiPSCs were checked for pluripotency markers, karyotype, CAG repeat length, and three germ layer differentiation. All hiPSC clones were registered at the Human Pluripotent Stem Cell Registry.

Patient-Derived Neural Progenitor Cells and Neuronal Cultures

For neuronal differentiation, hiPSCs were dissociated using accutase and resuspended in STEMdiff neural induction medium (NIM), including SMADi and Y-27632. The hiPSCs were replated in an AggreWell800 plate (all STEMCELL Technologies, Vancouver, Canada) and NIM was refreshed daily. After 7 days, embryoid bodies were transferred to a poly-D-lysine (PDL)/laminin-coated 6-well plate. Neural rosettes were selected using STEMdiff neural rosette selection reagent (STEMCELL Technologies) and replated in PDL/laminin-coated 6-well plates. After 7 days, Neural progenitor cells (NPCs) were passaged as single cells and expanded in STEMdiff neural progenitor medium (STEMCELL Technologies). Differentiation into neuronal cultures was done by plating 5×10^5 NPCs in a PDL/laminin-coated 6-well plate in

STEMdiff neuron differentiation medium. After 1 week, 5×10^5 cells were replated in PDL/laminin-coated 6-well plates in STEMdiff neuron differentiation medium, followed by half medium changes using BrainPhys medium every 2 to 3 days.

DNA Isolation and CAG Repeat Size Determination

DNA isolation and CAG repeat size determination were performed as reported before.^{21,34}

Mitochondrial Function

Using the Seahorse XF Extracellular Flux Analyzer XF96 (Agilent Technologies, Santa Clara, United States), oxygen consumption rate (OCR) was determined as a measure of mitochondrial respiration in fibroblasts and hiPSCs as described before.²¹

Immunohistochemistry

Cells were fixed with 4% paraformaldehyde (PFA) for 10 min at room temperature. Cells were pre-incubated for 1 h at room temperature in immunobuffer (100 μ L Triton X-100, 1 mL normal goat serum, 0.04 thimerosal in 100 mL Dulbecco's phosphate-buffered saline). Primary antibodies were diluted in immunobuffer and samples were incubated in a humidified chamber overnight at 4°C. Secondary antibodies were diluted in immunobuffer and samples were incubated for 2 hours at room temperature. Finally, samples were covered with Everbrite hardset containing 4', 6-diamidino-2-phenylindole (DAPI) (Biotum, USA). Antibody details can be found in Table 1.

Protein Aggregate Analysis

Images were obtained using a LeicaDMS5500. To avoid selection bias during image capturing, cells were selected by DAPI only. A total of 10 images per clone were obtained. Nuclear and cytoplasmic ataxin-1 aggregates were counted using the function "Cell counter" in ImageJ. The analysis was performed double blind.

Neuronal Morphology Analysis

Neurons were visualized using green fluorescent protein (GFP) transfection. For this, 2 μ L of Lipofectamine 2000 and 50 μ L Opti-MEM (Gibco) were incubated for 5 minutes at room temperature. Simultaneously, 1 μ g of pAcGFP1 plasmid and 50 μ L of Opti-MEM were incubated for 5 minutes at room temperature. Lipofectamine and DNA solutions were mixed and incubated for 20 minutes. This mixture was then added drop-wise onto the cells. After 4 hours, BrainPhys medium (Stemcell Technologies) was replaced. Cells were covered with Everbrite™ Hardset Mounting Medium containing

TABLE 1 *Antibodies*

Antibody	Species	Dilution	Company, catalog no., and RRID
2F5 ataxin-1	Mouse	1:250	Abbiotec, 253104, AB_11158080
MAP2	Mouse	1:500	Millipore, MAB364, AB_94948
β 3-tubulin	Mouse	1:200	Abcam, ab78078, AB_2256751
GFAP	Rabbit	1:500	Agilent, Z0334, AB_10013382
FOXG1	Rabbit	1:200	Abcam, ab196868, AB_2892604
VGluT1	Rabbit	1:200	Abcam, ab77822, AB_2187677
Synaptophysin	Rabbit	1:200	Abcam, ab52636, AB_882786
Ubiquitin	Rabbit	1:800	Agilent, Z0458, AB_2315524
Anti-mouse Alexa 488	Goat	1:500	Thermo Fisher Scientific, A-11001, AB_2534069
Anti-rabbit Alexa 594	Goat	1:500	Thermo Fisher Scientific, A-11012, AB_2534079

Abbreviation: MAP2, microtubule-associated protein; GFAP, glial fibrillary acidic protein; FOXG1, forkhead box protein G1; VGluT1, vesicular glutamate transporter 1.

DAPI (Biotum). Neurons were visualized using fluorescence microscopy (Leica, Germany). Using the ImageJ plugin NeuronJ, the length of processes emerging from the soma and the number of branches per cell soma were quantified. Analysis was performed double blind.

RNA Isolation and Real-Time Quantitative Reverse Transcription Polymerase Chain Reaction

RNA isolation and real-time quantitative reverse transcription polymerase chain reaction (RT-qPCR) was performed as described before.³² Primer details can be found in Table 2.

Multi-Electrode Array Recordings and Data Analysis

Data was analyzed using the multi-electrode array (MEA)-ToolBox to extract electrophysiological network parameters (Supplementary Methods and Hu et al.).³⁵

TABLE 2 *RT-qPCR primers*

Target gene	Primer name	Sequence (5'–3')
<i>ATXN1</i>	QPCR ATXN1 exon 3–4 F	ACTACAGGGAAGTGCATCAC
	QPCR ATXN1 exon 3–4 R	TGTTTCAAGACCATCCGTGC
<i>GFAP</i>	hGFAP_Fw1	ACCAGGACCTGCTCAATGTC
	hGFAP_Rev1	ATCTCCACGGTCTTACCAC
<i>MAP2</i>	hMAP2_Ex12_Fw1	TCCAAAATCGGATCAACAGA
	hMAP2_Ex13_Rev1	TGGATGTCACATGGCTTAGG

Abbreviation: RT-qPCR, real-time quantitative reverse transcription polymerase chain reaction.

Sequencing and Data Processing

Sequencing, differential gene expression analysis, gene enrichment analysis, and protein-protein interaction (PPI) network construction were performed using standard analysis pipelines (Supplementary Data S1 Methods).

Statistics

Statistical analysis was performed in GraphPad Prism 8 (GraphPad Software). Each data point within the analysis represents one well. The data was not normally distributed, as confirmed with a Shapiro–Wilk test. Therefore, the Mann–Whitney *U* test was used to test for significance. All data is represented as mean \pm standard error of mean (SEM). Only *P* values <0.05 were considered significant.

Data Sharing

Data is publicly available in the European Genome-Phenome Archive.

TABLE 3 Clinical information of the SCA1 patients and non-affected control individuals

Individuals	Cell line	Gender	Age at onset (range)	Average age at biopsy (range)	Average CAG repeat expanded allele (range)	Average SARA score (range)
4	Control	3 × F 1 × M		50 (44–54)		0.1 (0.0–0.5)
4	SCA1	3 × F 1 × M	38 (26–45)	42 (27–51)	46 (43–48)	10.3 (5.0–24.5)

Note: Table showing the gender, age at biopsy and when applicable, age at onset, self-reported CAG repeat length, and SARA score of patients and non-affected controls. Abbreviations: SCA1, spinocerebellar ataxia type 1; CAG, cytosine-adenine-guanine; F, female; M, male; SARA, scale for the assessment and rating of ataxia.

Results

SCA1 and Control Fibroblasts

SCA1 patients and non-affected family members were subjected to clinical evaluation. Three SCA1 patients had an age at onset in the fourth decade of life, whereas one patient had an age at onset already before age 30. All patients presented classic signs of SCA1. Patient 4 was in a more advanced state of the disease reflected by a high SARA score. The number of CAG repeats of the patients varied between 43 and 48. All clinical information is summarized in Table 3. Fibroblasts were cultured from skin biopsies. The CAG repeat length of all nine polyQ genes was determined and no disease-

causing repeat expansions were found (Supplementary Table S1).

Mitochondrial Dysfunction in Patient-Derived Fibroblasts

The *ATXN1* levels were examined in fibroblast samples and no difference was found between control and SCA1 fibroblasts (Fig. 1A). Because mitochondrial deficits were detected in several SCA1 models, we studied mitochondrial function (Fig. 1B). The SCA1 fibroblasts had significantly lower basal respiration and intracellular ATP levels compared to controls. However, these differences were mainly observed in fibroblasts obtained from

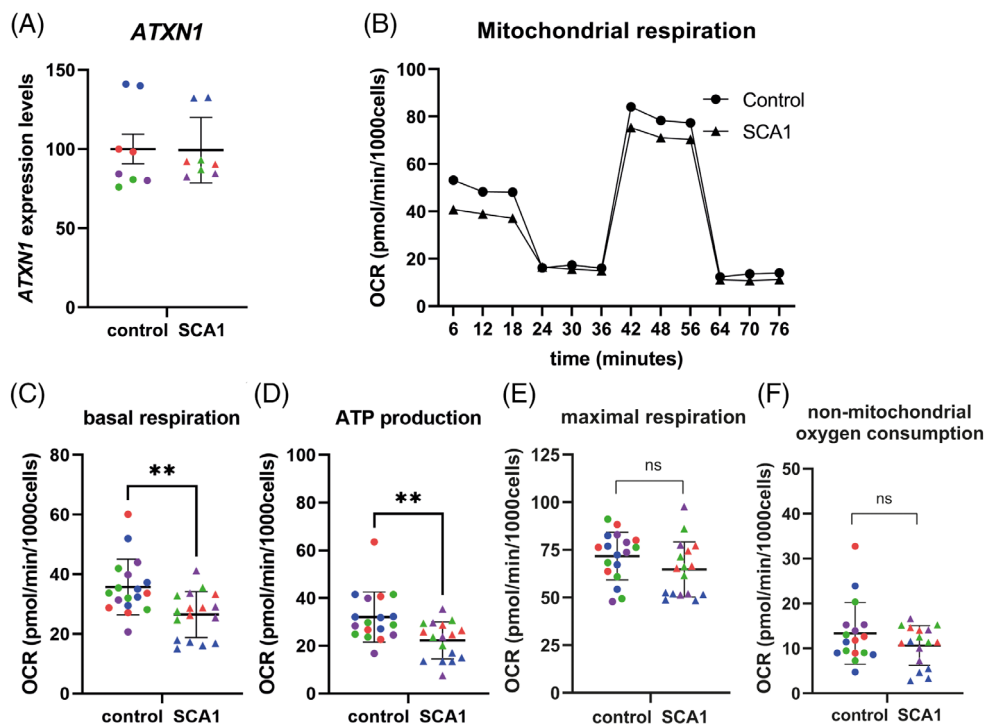


FIG. 1. Spinocerebellar ataxia type 1 (SCA1) patient-derived fibroblasts show a subtle decrease in mitochondrial respiration. (A) *ATXN1* is expressed in similar levels in control and patient-derived fibroblasts. (B) Representation of the mitochondrial stress test performed in control and SCA1 fibroblasts. (C) Basal respiration, (D) Adenosine triphosphate (ATP) production, (E) maximal respiration, and (F) non-mitochondrial oxygen consumption are derived from the mitochondrial stress test. A significant decrease is found in basal respiration ($P = 0.034$) and ATP production ($P = 0.0037$). No difference was found in maximal respiration and non-mitochondrial oxygen consumption. Average of two independent experiments, 4–6 replicates per control and SCA1 fibroblast line. Matching pairs are indicated with the same color. [Color figure can be viewed at wileyonlinelibrary.com]

TABLE 4 hiPSC clones derived from SCA1 patients and matched control individuals

Cell line	hiPSC clones (human pluripotent stem cell registry)
SCA1 1	LUMCi032-A and B
Control 1	LUMCi033-A, B and C
SCA1 2	LUMCi002-A, B and C
Control 2	LUMCi003-A and B
SCA1 3	LUMCi034-A, B and C
Control 3	LUMCi035-A, B and C
SCA1 4	LUMCi022-A, B and C
Control 4	LUMCi023-A

Note: Human pluripotent stem cell registry number of SCA1 patient and matched control hiPSC lines.

Abbreviations: SCA1, spinocerebellar ataxia type 1; hiPSC, human induced pluripotent stem cells.

the SCA1 patient with the earliest age at onset (blue pair, Fig. 1C,D). Maximal respiration and non-mitochondrial oxygen consumption were not different between SCA1 and control fibroblasts (Fig. 1E,F).

Generation, Characterization, and Differentiation of Patient-Derived hiPSCs

Previously, we published the generation of a SCA1 and a matched control hiPSC cell line.³² Here, we report the generation of three additional SCA1 patient-derived and matched control hiPSCs using non-integrating Sendai viruses, as described before (Table 4),^{32,36,37} In brief, all hiPSCs showed expression of pluripotency markers Oct3/4, Nanog, and SSEA-4 and were able to spontaneously differentiate into the three germ layers as shown by immunofluorescent staining for endodermal marker α -fetoprotein, mesodermal marker PECAM-1, and ectodermal marker β 3-tubulin. No chromosomal aberrations were found and all hiPSCs clones were Sendai virus and mycoplasma free.

NPCs were generated using a standard protocol (Fig. 2A). Differentiation of NPCs resulted in stable neuronal cultures containing both neurons and astrocytes. Cultures were stained with neuronal marker microtubule-associated protein 2 (MAP2) and astrocyte marker glial fibrillary acidic protein (GFAP). No differences in the ratio of neuronal cells and glial cells were observed between the hiPSC clones (Fig. 2B), as confirmed by quantitative reverse transcription PCR (RT-qPCR) (Fig. 2C,D). The cultures stain positive for FOXG1 (cortical lineage), β 3tubulin, synaptophysin, and vGlut. No differences in expression of excitatory and inhibitory markers were seen between the SCA1 and control cultures (Supplementary Fig. S1). Moreover, no

differences in *ATXN1* levels were observed, confirming that the phenotypes in downstream assays were because of the repeat expansion rather than to altered *ATXN1* expression levels (Fig. 2E).

Mitochondrial Dysfunction in SCA1 Patient-Derived Neuronal Cultures

Next, we investigate whether the mitochondrial phenotype found in fibroblasts was also present in patient-derived neuronal cultures. SCA1 patient-derived neuronal cultures had significantly lower basal and maximal respiration levels and lower intracellular ATP levels compared to controls. Non-mitochondrial oxygen consumption was comparable between both conditions (Fig. 3A–E). In contrast to the fibroblast experiments, a robust difference was observed in all SCA1 patient-derived neuronal cultures.

Altered Electrophysiology in SCA1 Patient-Derived Neuronal Cultures

A MEA was used to study changes in fire rate, single-channel burst (SCB) activity and neuronal network activity (Fig. 3F–H), which is visualized at three time windows: (1) at DIV1-23 the network activity was similar between both groups; (2) at DIV23-40 the SCA1 cultures showed a decrease in network bursts compared to controls; and (3) at DIV40-60 a similar network activity was observed for both conditions (Fig. 3H). We analyzed the network bursts at time points DIV8, DIV33, and DIV60 (Fig. 3I–K). On DIV8 and DIV60, there was no difference in the amount of network bursts between groups, whereas on DIV33 a significant decrease in both the number and the duration of network bursts was observed in the SCA1 group compared to controls. However, these shorter network bursts were more regular compared to controls. Similar trends could be seen in representative spike raster plots (Fig. 3I–K). Taken together, these data demonstrate a delay in network development in SCA1 hiPSC-derived neuronal cultures.

Nuclear and Cytoplasmic Aggregates in SCA1 Patient-Derived Neuronal Cultures

Protein aggregation is one of the main pathophysiological hallmarks of SCA1. We examined the presence of aggregates in fibroblasts and hiPSC-derived neurons after 2, 4, and 6 weeks of neuronal maturation. No aggregates were observed in SCA1 fibroblasts. Instead, after 2 weeks of neuronal maturation, SCA1 neuronal cultures showed a significantly higher percentage of cells with intranuclear aggregates and a higher number of aggregates per cell compared to controls. These numbers increased significantly over time in patient-derived neuronal cultures (Fig. 4A,B). Aggregates were not only found in the nucleus, but also in the

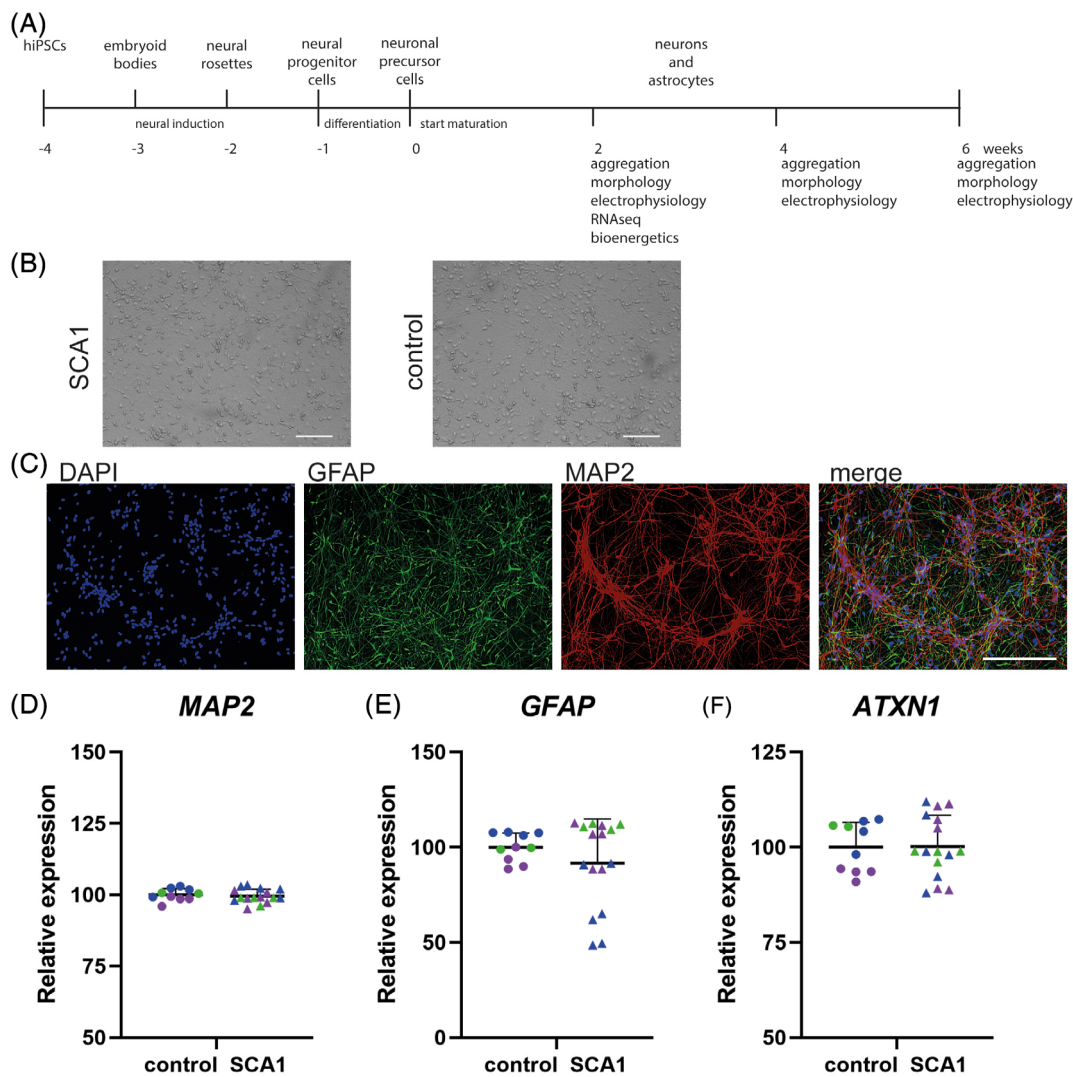


FIG. 2. Neuronal differentiation of control and spinocerebellar ataxia type 1 (SCA1) human induced pluripotent stem cells (hiPSCs) is comparable. **(A)** Outline of the neuronal differentiation protocol. **(B)** Representative bright field images of 2-week-old hiPSCs neuronal cultures derived from control and SCA1. **(C)** Neurons are stained with the nuclear marker 4', 6-diamidino-2-phenylindole (blue), the astrocyte marker glial fibrillary acidic protein (GFAP) (green) and the neuronal marker MAP2 (red). The scale bar is 100 μm. **(D–F)** Q-RT-PCR results showing similar levels of the neuronal marker MAP2, the astrocyte marker GFAP and ATXN1. Per fibroblast line 1–3 independent clones were generated. All clones were analyzed in two independent, biological replicates. Matching pairs are indicated in the same color. [Color figure can be viewed at wileyonlinelibrary.com]

cytoplasm of SCA1 neuronal cultures. Similarly, both the percentage of cells containing a cytoplasmic aggregate and the number of cytoplasmic aggregates per cell increased significantly over time in patient-derived neuronal cultures (Fig. 4C,D).

Nuclear and Cytoplasmic Aggregates in SCA1 Post-Mortem Brain Tissue

Studies investigating protein aggregation in SCA1 post-mortem brain tissue mostly report on intranuclear aggregates. Because the hiPSC-derived neuronal cultures also showed cytoplasmic aggregates, we determined the localization of the aggregates in SCA1 post-mortem brain tissue. Macroscopically we observed typical hallmarks of SCA1, which is atrophy of the cerebellum,

pontine nucleus, and medulla oblongata. Furthermore, we observed atrophy of the caudate nucleus. On microscopical examination, neuronal loss and gliosis was mostly observed in the pontine nucleus, olivary nucleus, and PC layer of the cerebellum. Nuclear and cytoplasmic ubiquitin-positive aggregates were found throughout the brain, but mostly in the pontine nucleus and olivary nucleus (Fig. 4E,F).

Altered Morphology in SCA1 Patient-Derived Neuronal Cultures

Ataxin-1 is a transcriptional regulator for genes involved in neuronal connectivity and differentiation. Proper synaptic contacts with neighboring cells are essential for the development and complexity of

neuronal cell dendritic trees. Neuronal morphology can be used as a measure for dendritic tree complexity. Process length and the number of branching points were analyzed in GFP-transfected neurons

after 2, 4, and 6 weeks of neuronal maturation (Fig. 4G).

In SCA1 neurons, process length were significantly shorter compared to that in control neurons across all

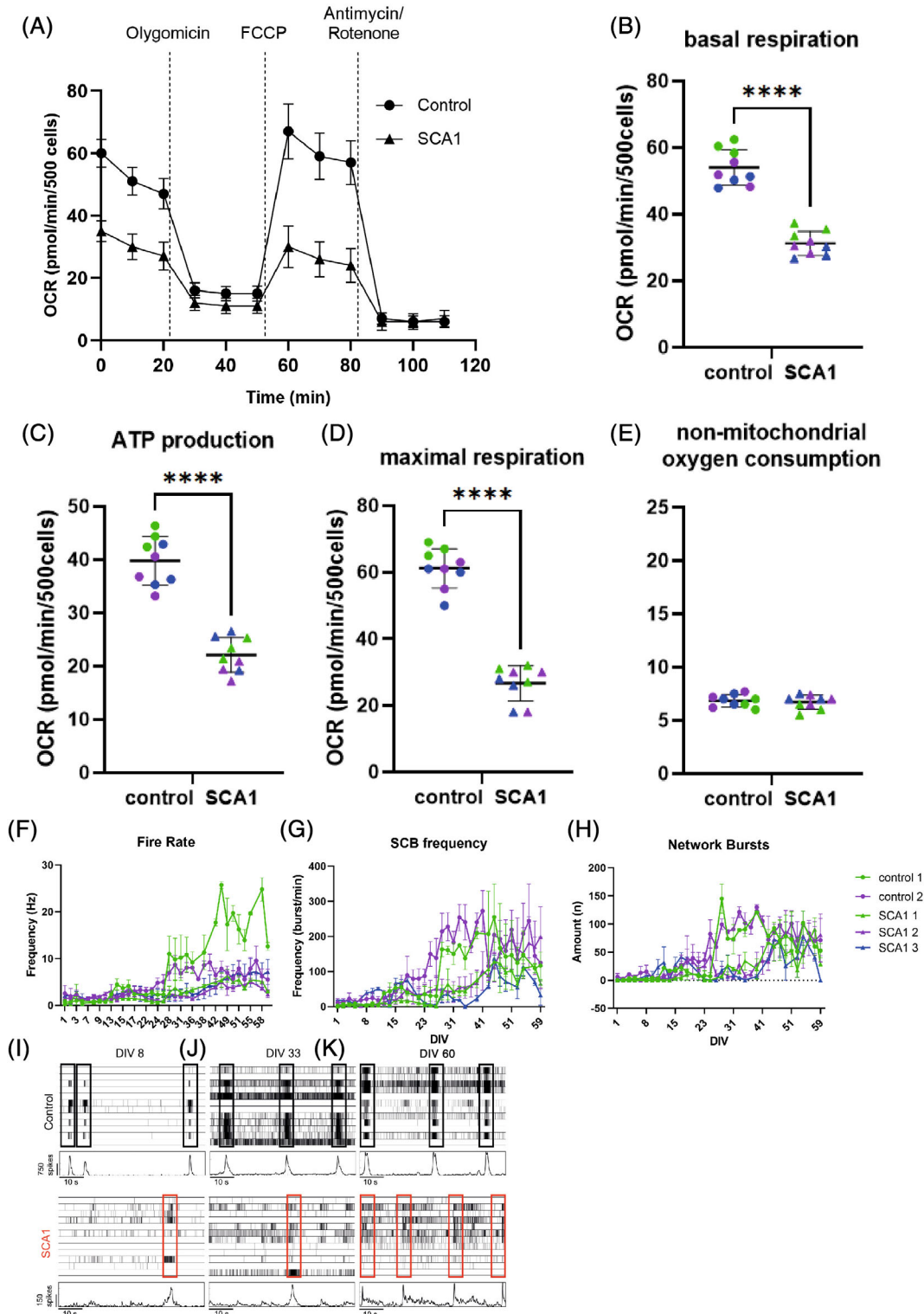


FIG. 3. Legend on next page.

time points. Furthermore, process length in SCA1 neurons did not increase over time, whereas process length in control neurons increased over time (Fig. 4I). As a further indicator of process complexity, we measured the number of branching points. There were significantly less branching points in SCA1 cultures compared to controls. No increase in number of branching points was seen over time in either condition (Fig. 4J). Overall, these results indicate that dendritic length and complexity are decreased in SCA1 neurons.

Functional Analysis of Dysregulated Genes in SCA1 Patient-Derived Neuronal Cultures

To confirm known deregulated pathways and discover novel SCA1 disease pathways, we performed RNA-seq. After filtering and data normalization, 15,644 genes were included. Data was normally distributed after log2CPM transformation and principle component analysis showed no outliers and a clear separation between SCA1 and control samples (Supplementary Fig. S2A,B). Independent differential gene expression analysis was performed in each patient and matched control individual dataset. A total of 1236 differentially expressed genes (DEGs) overlapped with 1050 DEGs deregulated in the same direction (Fig. 5A,B). The number of up- and down-regulated DEGs was similar per dataset (Supplementary Fig. S2C and Fig. 5C). We sorted the 1050 DEGs on adjusted *P*-value or logFC to prioritize genes with the most extreme changes (Fig. 5D and Supplementary Fig. S2D,E). For technical validation, we selected genes from the top 25 DEGs that were expressed at high enough levels and were previously associated with SCA, neurodegeneration or neurodevelopment, confirming disease relevant changes (Supplementary Table S2).

Capicua (CIC) is an evolutionarily conserved transcription factor binding to ataxin-1. The interaction of mutant ataxin-1 with CIC mediates toxicity in SCA1 models.³⁸ We found significantly increased *CIC* RNA levels in SCA1 neurons, as previously shown in an independent dataset from a human overexpression model of *ATXN1(Q82)*.³⁹ Furthermore, several *CIC* target genes, including *ETV5*, *CCNE1*, *DUSP6*, and *PER2*

were dysregulated in SCA1 cultures (Supplementary Fig. S2F–L).

We performed gene set enrichment analysis to identify enriched biological mechanisms by annotating the DEGs for Kyoto Encyclopedia of Genes and Genomes pathway analysis, Gene Ontology (GO) biological processes (BP) and cellular components (CC). Processes related to synapse organization, neuron projection guidance, and axon development were positively regulated, confirming disease relevant changes. In contrast, regulation of cell cycle, DNA replication, and repair and organelle fission were negatively regulated, consistent with previous findings in both cells and SCA1 human cerebellum³⁹ (Fig. 5E). Functional analysis from the annotation with GO CC identified genes related to the synaptic membrane, mitotic spindle, and mitochondrial matrix (Supplementary Fig. S2M). Dysregulated pathways included axon guidance, cell cycle, calcium, and p53 signaling pathways (Supplementary Fig. S2N).

Protein–Protein Interaction Networks Highlight Central Aspects of SCA1 Pathology

Next, we generated a protein–protein interaction network consisting of 924 nodes and further subjected this network to clustering analysis for visualization and detection of protein communities with similar functional similarities and high connectivity centralities. The network consisted of four major clusters (Fig. 5F and Supplementary Fig. S3); community cluster 1 (CC1) was the biggest containing 151 nodes. Based on their centrality values, RhoA and mitogen-activated protein kinase 1 (MAPK1) were the central nodes, suggesting that they are key regulators of the information flow within CC1 (Fig. 5F). The components of CC1 are involved in several signaling pathways, including MAPK, Ras, oxytocin, and Ca²⁺ signaling and processes related to neurotransmitter secretion and transport (Fig. 5G). These signaling pathways are interconnected and their functionality may be regulated by common kinases, such as protein kinase C (PKC), which is significantly dysregulated in the SCA1 neuronal cultures (Supplementary Fig. S4).

FIG. 3. Robust functional differences in mitochondrial respiration and multi-electrode array between control and spinocerebellar ataxia type 1 (SCA1) human induced pluripotent stem cell (hiPSC)-derived neuronal cultures. **(A)** Representation of the mitochondrial stress test performed in 2-week-old control and SCA1 hiPSC-derived neurons. **(B)** Basal respiration, **(C)** adenosine triphosphate (ATP) production, **(D)** maximal respiration, and **(E)** non-mitochondrial oxygen consumption are derived from the mitochondrial stress test. Significant differences are found in basal respiration ($P < 0.001$), ATP production ($P < 0.001$), and maximal respiration ($P < 0.001$). Matching pairs are indicated in the same color. Longitudinal recordings of network activity of controls and SCA1 neurons for 60 days in vitro (DIVs), **(F–H)** we observed three time windows in the longitudinal recordings of network activity and selected one representative day for each of these time windows (DIV 8, DIV 33, and DIV 60). The network activity on DIV 8 and DIV 60 are not significantly different between control and SCA1 groups, but on DIV 33 the network activity was significantly different between control and SCA1 groups (**Supplementary figure XA**). Furthermore, when looking at the network burst activity of the SCA1 neurons on DIV 33 these network bursts are shorter (**Supplementary figure XB**) and more regular (**Supplementary figure XC**) when compared to those of the control group. Similar trends can also be seen in the spike raster plots between the control and SCA groups, with inserts highlighting network burst activity in each raster plot, and spike histograms showing bursting patterns between control and SCA neuronal cultures. **(I–K)** The detected network bursts are highlighted in black (control) or red (SCA1). Beneath the raster plots are spike histograms in which each peak represents a network burst to help identifying network bursting patterns. [Color figure can be viewed at wileyonlinelibrary.com]

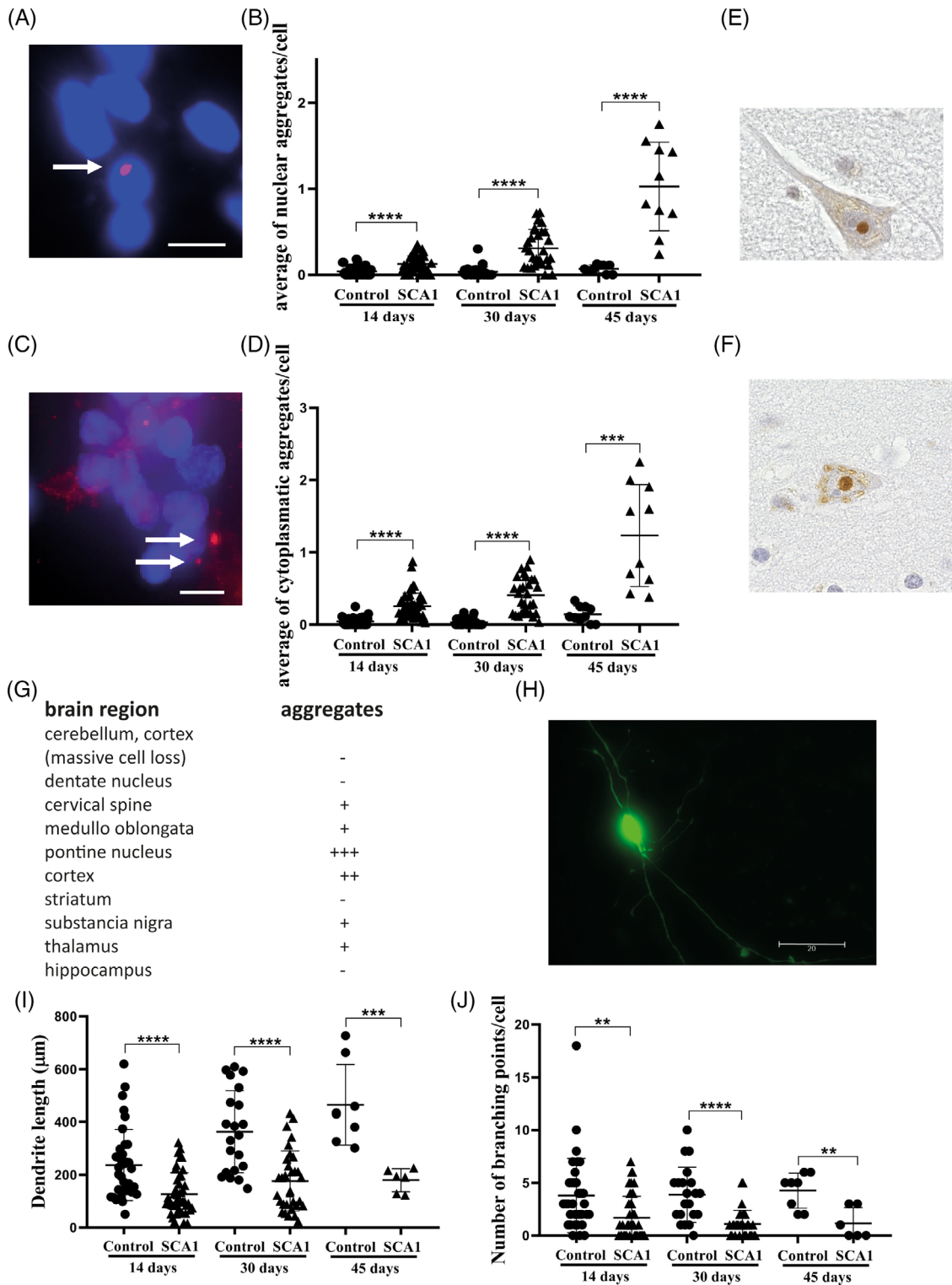


FIG. 4. Protein aggregation and morphological differences between control and (spinocerebellar ataxia type 1) SCA1 human induced pluripotent stem cells (hiPSC)-derived neuronal cultures. **(A)** Immunohistochemistry of hiPSC-derived neurons of controls and SCA1 at 2, 4, and 6 weeks. Cells were stained with 4', 6-diamidino-2-phenylindole (blue) and ataxin-1 (red). Scale bar is 10 μ m. Intranuclear protein aggregates in hiPSC-derived neuronal cultures. **(B)** Quantification of intranuclear protein aggregates in control and SCA1 neuronal cultures. **(C)** Cytoplasmic protein aggregates in hiPSC-derived neuronal cultures. **(D)** Quantification of cytoplasmic protein aggregates in control and SCA1 neuronal cultures. Number of cell lines per time point: 14 days (control n = 3, SCA1 n = 3), 30 days (control n = 3, SCA1 n = 3), and 45 days (control n = 1, SCA1 n = 1). * P < 0.05, ** P < 0.01, *** P < 0.001, **** P < 0.0001 by *t*-test, one-way ANOVA and Sidak's multiple comparison test **(E)** intranuclear and **(F)** cytoplasmic aggregates in SCA1 post mortem brain tissue **(G)** quantification of aggregates in post-mortem brain tissue **(H)** neurons transfected with a green fluorescent protein construct to measure **(I)** dendrite length and **(J)** the number of branch points. [Color figure can be viewed at wileyonlinelibrary.com]

More importantly, overrepresentation analysis using the rare disease-dedicated platform Orphanet indicated that CC1 is highly associated with cerebellar ataxia, confirming its relevance with SCA1 pathology (Supplementary Fig. S5). The other major community clusters, CC2, CC3, and CC4 are involved in metabolism, cell cycle, and protein processing, respectively. Centrality analysis indicated that these clusters contain novel candidate targets, including fumarate hydratase (FH) and aconitase 2 (ACO2) in CC2, anillin (ANLN), and thymidylate synthase (TYMS) in CC3, general vesicular transport factor p115 (USO1) and transmembrane p24 trafficking protein 10 (TMED10) in CC4. Taken together, these results suggest that these clusters might have a critical impact in SCA1 pathology.

Discussion

Mitochondrial alterations have been described in SCA1 in terms of morphology and functionality by changes in electron transport chain complexes and lower ATP production.^{23,25,40} Here, we found that energy metabolism was altered in SCA1 fibroblasts and patient-derived neurons. The differences in SCA1 fibroblasts were minor compared to those found in SCA1 neuronal cultures and mainly caused by one fibroblast line. An explanation might be the severe disease stage of this particular patient, as indicated by the high SARA score. Mitochondrial dysfunction has been associated with many repeat expansion neurodegenerative diseases, including polyQ SCAs, HD, and fragile X-associated tremor/ataxia syndrome (FXTAS).^{21,23,25,40-42} We have previously shown that energy metabolism in HD fibroblasts was associated with age at onset independent of the CAG repeat expansion.²¹ The fact that we can detect mitochondrial changes in SCA1 fibroblasts is intriguing and supports the use of patient-derived fibroblasts in the development of therapeutic interventions. Mitochondrial changes were further confirmed in SCA1 hiPSC-derived neurons. Altered cellular metabolism is believed to be an important contributor to pathogenesis of polyQ disorders, including HD. Decreased ATP levels and maximal respiration were found in HD, SCA2, and SCA3 hiPSC-derived cells across differentiation stages and protocols.^{30,41} These findings are in line with previous studies, indicating that SCA1 disease pathogenesis involves mitochondrial deficits.^{23,25,40}

SCA1 is characterized by a widespread neuronal dysfunction; however, the underlying pathogenic mechanisms are still elusive. One of the main hallmarks of the disease is protein aggregates in post-mortem brain tissue. Accumulation of aggregates is suggested to correlate with a gradual decline in proteostasis and is promoted by aging. Although protein aggregation is a characteristic feature, it is still questionable whether

protein aggregates directly contribute to disease pathogenesis or merely represent a cellular strategy to protect cells from toxic effects of expanded polyQ proteins. Studies in post mortem human polyQ SCA brain tissue suggest a lack of correlation between the presence of aggregates in different brain regions and the severity of neurodegeneration.^{15,55,56} However, studies using SCA1 mouse models and overexpression cell models indicate that SCA1 disease progression is associated with the gradual accumulation of protein aggregates. Here, SCA1 patient-derived neuronal cultures show ataxin-1 positive aggregates, which increased significantly in number over time. Most studies in post-mortem brain tissue report intranuclear, but also cytoplasmic, protein aggregates in SCA1 overexpression models.⁴³ In the current study, the presence of cytoplasmic protein aggregates was validated in SCA1 brain tissue. In Neuro-2a cells, the interactome of ataxin-1 [85Q] revealed a significant enrichment of essential nuclear transporters, suggesting that elevated levels of ataxin-1 correlate with disruptions in nuclear transport processes. Electron microscopy studies have shown that perinuclear aggregates are associated with a typical distortion of the nuclear surface. However, only few studies report the state of the nuclear envelope adjacent to protein aggregates. Disruption of the nuclear envelope has been implicated in other repeat expansion disorders, including HD and FXTAS. Interestingly, from a mechanistic perspective, cell toxicity observed in FXTAS can be rescued on overexpression of the lamina-associated protein LAP2 β .⁵³ The pathological features, including polyQ aggregation and mitochondrial dysfunction, can be recapitulated in disease-derived hiPSC neurons from SCA2, SCA3, and FXTAS patients.^{28,30,44}

Mutant ataxin-1 causes anatomical abnormalities in the developing cerebellum¹⁷ as well as a loss of complexity and branching in the PC dendritic trees of SCA1 animals.¹⁶ Although PCs are the most affected cell type in SCA1, it has been shown that other cells, including forebrain neurons, are affected in SCA1 animal models. These forebrain neurons require ataxin-1 for proper development and connectivity.⁴⁵ Similar to many of the known affected neurons in SCA1 animal models (eg, PCs, vestibular, and substantia nigra neurons),⁴⁶⁻⁴⁹ forebrain neurons have also been described to have a pacemaker-like function.⁵⁰ The mixed cultures used in this study lack Purkinje neurons and Bergman glia, which are highly specialized cerebellar cells. A one to one comparison of the MEA data with Purkinje neuron pacemaker firing is, therefore, not feasible; however, the data reveals that neurons carrying ataxin-1 mutation also harbor electrophysiological changes. Our results suggest there is an intrinsic defect in neuronal development because both process length and branching complexity were altered in SCA1 hiPSC-

derived neurons. Genes related to synapse organization, neuron projection development, and axon guidance were enriched in the GO analysis. In the cerebellum, synapses with parallel fibers as well as climbing fibers are necessary for the development and maturation of PCs. In SCA1 mice, early expression of mutant ataxin-1 caused climbing fiber-PC deficiencies early in life, before symptom onset.⁵¹ This highlights the importance of impaired connectivity in the early pathophysiology of SCA1. The loss of synaptic contacts is because of abnormal synaptic architecture and signaling caused by the lack of activity of ataxin-1 as a transcriptional regulator. Synaptic protein scaffold loss in SCA1 was observed before the onset of symptoms.⁵²

Electrophysiological data showed that SCA1 network activity is delayed, hinting toward developmental issues present within the SCA1 neurons electrical firing. The MEA data from the first 40 days are in line with several other neurodevelopmental and neurodegenerative disorders showing altered neuronal network dynamics in hiPSC-derived neuronal cultures.^{53,54}

In SCA1 and SCA2 mouse models, it has been shown that the PCs have reduced cell excitability expressed as a lower basal pacemaker firing, which precedes any structural change or motor dysfunction.^{55,56} Interestingly, in transgenic SCA3 mouse model, there is an increase in cell excitability leading to a depolarization block. This results in PCs unable to fire, similarly to the SCA1 and SCA2 mouse models.⁵⁷ This eventual reduction in the capability of PCs to fire properly and repetitively, could be a common functional endpoint seen with polyQ disorders.⁵⁸

However, our data show that the reduced network activity is temporary. One of the early characteristics of the SCA pathology is neuronal atrophy followed eventually by neuronal cell death. A potential explanation for this spontaneous “recovery” could lie in that the neuronal atrophy, at least in the early stages of the disease, might actually be a compensatory mechanism, which tries to maintain normal neuronal function. In SCA1 mice, it has been shown that the reduced basal pacemaker firing of PCs causes neuronal atrophy. Subsequently, the neuronal atrophy then allows the PCs to maintain the appropriate density of potassium channels to restore the disturbed pacemaker firing of the PCs.⁵⁹ This mechanism might explain the spontaneous recovery observed in the electrophysiological data of the SCA1 cell lines.

Previously, a computational approach was used to identify dysregulated pathways and genes regulated by CIC, the main driver of pathogenesis in SCA1. The analysis highlighted the important role of MAPK1 and RhoA in an in vitro and in vivo SCA1 protein aggregation model.⁶⁰ Remarkably, expression of *MAPK1* (*ERK2*) and *RHOA* genes was significantly downregulated in SCA1 hiPSC-derived neurons, whereas their protein products constitute the major components of the disease-

relevant CC1. CIC acts as a transcriptional repressor of genes regulated by the MAPK/ERK signaling pathway,⁶¹ whereas phosphorylation and degradation of CIC by MAPK/ERK induces histone acetylation and prolonged translational repression.^{62,63} The pathological ATXN1-CIC axis may repress the MAPK/ERK pathway generating a negative feedback loop.⁶⁴ This repression may be also because of the dysregulation of the upstream calcium and Ras signaling pathways through common kinases, including PKC, which is involved in the proper function of Purkinje neurons.⁶⁵ Furthermore, the network analysis indicates novel genes, including FH and ACO2, which regulate the function of CC2 and are directly involved in mitochondrial energy production. These results suggest that FH and ACO2 might be responsible for the robust functional differences in mitochondrial respiration of SCA1 patient-derived neurons.

Altogether, SCA1 patient-specific neuronal cultures recapitulate key pathological features of this disease, including mitochondrial dysfunction, protein aggregation, altered neuronal morphology, and an abnormal electrophysiological profile. The SCA1 neuronal model can be used for the identification of compounds that may prevent or rescue neurodegeneration in this devastating disease, including RNA targeting therapies and intervention strategies based on newly identified pathways. ■

Acknowledgments: We thank the SCA1 patients united in the Dutch SCA1 families fund for their contribution in the project.

Ethics Approval and Consent to Participate

This study was approved by the LUMC medical ethics committee (NL45478.058.13/P13.080) and written informed consent was obtained from all participants.

Consent for Publication

All individuals participating in this study signed an informed consent form.

Data Availability Statement

The data that supports the findings of this study are available in the supplementary material of this article.

References

1. Sullivan R, Yau WY, O'Connor E, Houlden H. Spinocerebellar ataxia: an update. *J Neurol* 2019;266(2):533–544.
2. Schols L, Bauer P, Schmidt T, Schulte T, Riess O. Autosomal dominant cerebellar ataxias: clinical features, genetics, and pathogenesis. *Lancet Neurol* 2004;3(5):291–304.
3. Opal P, Ashizawa T. Spinocerebellar ataxia type 1. In: Adam MP, Ardinger HH, Pagon RA, Wallace SE, Bean LJJ, Stephens K, et al., eds. *GeneReviews*(R). Seattle, WA: University of Washington,

- Seattle. GeneReviews is a registered trademark of the University of Washington, Seattle. All rights reserved.; 1993.
4. Jacobi H, Bauer P, Giunti P, Labrum R, Sweeney MG, Charles P, et al. The natural history of spinocerebellar ataxia type 1, 2, 3, and 6: a 2-year follow-up study. *Neurology* 2011;77(11):1035–1041.
 5. Zoghbi HY, Pollack MS, Lyons LA, Ferrell RE, Daiger SP, Beaudet AL. Spinocerebellar ataxia: variable age of onset and linkage to human leukocyte antigen in a large kindred. *Ann Neurol* 1988;23(6):580–584.
 6. Orr HT, Chung MY, Banfi S, Kwiatkowski TJ Jr, Servadio A, Beaudet AL, et al. Expansion of an unstable trinucleotide CAG repeat in spinocerebellar ataxia type 1. *Nat Genet* 1993;4(3):221–226.
 7. Goldfarb LG, Vasconcelos O, Platonov FA, Lunkes A, Kipnis V, Kononova S, et al. Unstable triplet repeat and phenotypic variability of spinocerebellar ataxia type 1. *Ann Neurol* 1996;39(4):500–506.
 8. Zuhlke C, Dalski A, Hellenbroich Y, Bubel S, Schwinger E, Burk K. Spinocerebellar ataxia type 1 (SCA1): phenotype-genotype correlation studies in intermediate alleles. *Eur J Med Genet* 2002;10(3):204–209.
 9. Buijsen RAM, Toonen LJA, Gardiner SL, van Roon-Mom WMC. Genetics, mechanisms, and therapeutic progress in polyglutamine spinocerebellar ataxias. *Neurotherapeutics* 2019;16(2):263–286.
 10. Paulson HL, Shakkottai VG, Clark HB, Orr HT. Polyglutamine spinocerebellar ataxias—from genes to potential treatments. *Nat Rev Neurosci* 2017;18(10):613–626.
 11. Fan HC, Ho LI, Chi CS, Chen SJ, Peng GS, Chan TM, et al. Polyglutamine (PolyQ) diseases: genetics to treatments. *Cell Transplant* 2014;23(4–5):441–458.
 12. Seidel K, Siswanto S, Brunt ER, den Dunnen W, Korf HW, Rub U. Brain pathology of spinocerebellar ataxias. *Acta Neuropathol* 2012;124(1):1–21.
 13. Duyckaerts C, Durr A, Cancel G, Brice A. Nuclear inclusions in spinocerebellar ataxia type 1. *Acta Neuropathol* 1999;97(2):201–207.
 14. Watase K, Weeber EJ, Xu B, Antalffy B, Yuva-Paylor L, Hashimoto K, et al. A long CAG repeat in the mouse SCA1 locus replicates SCA1 features and reveals the impact of protein solubility on selective neurodegeneration. *Neuron* 2002;34(6):905–919.
 15. Zu T, Duvick LA, Kaytor MD, Berlinger MS, Zoghbi HY, Clark HB, et al. Recovery from polyglutamine-induced neurodegeneration in conditional SCA1 transgenic mice. *J Neurosci* 2004;24(40):8853–8861.
 16. Edamakanti CR, Do J, Didonna A, Martina M, Opal P. Mutant ataxin1 disrupts cerebellar development in spinocerebellar ataxia type 1. *J Clin Invest* 2018;128(6):2252–2265.
 17. Ibrahim MF, Power EM, Potapov K, Empson RM. Motor and cerebellar architectural abnormalities during the early progression of ataxia in a mouse model of SCA1 and how early prevention leads to a better outcome later in life. *Front Cell Neurosci* 2017;11:292.
 18. Seong IS, Ivanova E, Lee JM, Choo YS, Fossale E, Anderson M, et al. HD CAG repeat implicates a dominant property of huntingtin in mitochondrial energy metabolism. *Hum Mol Genet* 2005;14(19):2871–2880.
 19. Siddiqui A, Rivera-Sanchez S, Castro Mdel R, Acevedo-Torres K, Rane A, Torres-Ramos CA, et al. Mitochondrial DNA damage is associated with reduced mitochondrial bioenergetics in Huntington's disease. *Free Radic Biol Med* 2012;53(7):1478–1488.
 20. Cornelius N, Wardman JH, Hargreaves IP, Neerghen V, Bie AS, Tumer Z, et al. Evidence of oxidative stress and mitochondrial dysfunction in spinocerebellar ataxia type 2 (SCA2) patient fibroblasts: effect of coenzyme Q10 supplementation on these parameters. *Mitochondrion* 2017;34:103–114.
 21. Gardiner SL, Milanese C, Boogaard MW, Buijsen RAM, Hogenboom M, Roos RAC, et al. Bioenergetics in fibroblasts of patients with Huntington disease are associated with age at onset. *Neurol Genet* 2018;4(5):e275.
 22. Ward JM, Stoyas CA, Switonski PM, Ichou F, Fan W, Collins B, et al. Metabolic and organelle morphology defects in mice and human patients define spinocerebellar ataxia type 7 as a mitochondrial disease. *Cell Rep* 2019;26(5):1189–1202.
 23. Stucki DM, Rueggsegger C, Steiner S, Radecke J, Murphy MP, Zuber B, et al. Mitochondrial impairments contribute to spinocerebellar ataxia type 1 progression and can be ameliorated by the mitochondria-targeted antioxidant MitoQ. *Free Radic Biol Med* 2016;97:427–440.
 24. Sanchez I, Balague E, Matilla-Duenas A. Ataxin-1 regulates the cerebellar bioenergetics proteome through the GSK3beta-mTOR pathway which is altered in spinocerebellar ataxia type 1 (SCA1). *Hum Mol Genet* 2016;25(18):4021–4040.
 25. Ferro A, Carbone E, Zhang J, Marzouk E, Villegas M, Siegel A, et al. Short-term succinic acid treatment mitigates cerebellar mitochondrial OXPHOS dysfunction, neurodegeneration and ataxia in a Purkinje-specific spinocerebellar ataxia type 1 (SCA1) mouse model. *PLoS One* 2017;12(12):e0188425.
 26. Takahashi K, Tanabe K, Ohnuki M, Narita M, Ichisaka T, Tomoda K, et al. Induction of pluripotent stem cells from adult human fibroblasts by defined factors. *Cell* 2007;131(5):861–872.
 27. Hommersom MP, Buijsen RAM, van Roon-Mom WMC, van de Warrenburg BPC, van Bokhoven H. Human induced pluripotent stem cell-based modelling of spinocerebellar ataxias. *Stem Cell Rev Rep* 2021;18(2):441–456.
 28. Koch P, Breuer P, Peitz M, Jungverdorben J, Kesavan J, Poppe D, et al. Excitation-induced ataxin-3 aggregation in neurons from patients with Machado-Joseph disease. *Nature* 2011;480(7378):543–546.
 29. Ishida Y, Kawakami H, Kitajima H, Nishiyama A, Sasai Y, Inoue H, et al. Vulnerability of Purkinje cells generated from spinocerebellar ataxia type 6 patient-derived iPSCs. *Cell Rep* 2016;17(6):1482–1490.
 30. Chuang CY, Yang CC, Soong BW, Yu CY, Chen SH, Huang HP, et al. Modeling spinocerebellar ataxias 2 and 3 with iPSCs reveals a role for glutamate in disease pathology. *Sci Rep* 2019;9(1):1166.
 31. Scholefield J, Watson L, Smith D, Greenberg J, Wood MJ. Allele-specific silencing of mutant Ataxin-7 in SCA7 patient-derived fibroblasts. *Eur J Hum Genet* 2014;22(12):1369–1375.
 32. Buijsen RAM, Gardiner SL, Bouma MJ, van der Graaf LM, Boogaard MW, Pepers BA, et al. Generation of 3 spinocerebellar ataxia type 1 (SCA1) patient-derived induced pluripotent stem cell lines LUMCi002-A, B, and C and 2 unaffected sibling control induced pluripotent stem cell lines LUMCi003-A and B. *Stem Cell Res* 2018;29:125–128.
 33. Schmitz-Hubsch T, du Montcel ST, Baliko L, Berciano J, Boesch S, Depondt C, et al. Scale for the assessment and rating of ataxia: development of a new clinical scale. *Neurology* 2006;66(11):1717–1720.
 34. Gardiner SL, Harder AVE, Campman YJM, Trompet S, Gussekloo J, van Belzen MJ, et al. Repeat length variations in ATXN1 and AR modify disease expression in Alzheimer's disease. *Neurobiol Aging* 2019;73:230.e9–230.e17.
 35. Hu M, Frega M, Tolner EA, van den Maagdenberg A, Frimat JP, le Feber J. MEA-toolbox: an open source toolbox for standardized analysis of multi-electrode array data. *Neuroinformatics* 2022;20(4):1077–1092.
 36. Daoutsali E, Buijsen RAM, van de Pas S, Jong A, Mikkers H, Brands T, et al. Generation of 3 human induced pluripotent stem cell lines LUMCi005-A, B and C from a hereditary cerebral hemorrhage with amyloidosis-dutch type patient. *Stem Cell Res* 2019;34:101359.
 37. van der Graaf LM, Gardiner SL, Tok M, Brands T, Boogaard MW, Pepers BA, et al. Generation of 5 induced pluripotent stem cell lines, LUMCi007-A and B and LUMCi008-A, B and C, from 2 patients with Huntington disease. *Stem Cell Res* 2019;39:101498.
 38. Fryer JD, Yu P, Kang H, Mandel-Brehm C, Carter AN, Crespo-Barreto J, et al. Exercise and genetic rescue of SCA1 via the transcriptional repressor capicua. *Science* 2011;334(6056):690–693.
 39. Laidou S, Alanis-Lobato G, Pribyl J, Rasko T, Tichy B, Mikulasek K, et al. Nuclear inclusions of pathogenic ataxin-1 induce oxidative stress and perturb the protein synthesis machinery. *Redox Biol* 2020;32:101458.

40. Tichanek F, Salomova M, Jedlicka J, Kuncova J, Pitule P, Macanova T, et al. Hippocampal mitochondrial dysfunction and psychiatric-relevant behavioral deficits in spinocerebellar ataxia 1 mouse model. *Sci Rep* 2020;10(1):5418.
41. Consortium THi. Bioenergetic deficits in Huntington's disease iPSC-derived neural cells and rescue with glycolytic metabolites. *Hum Mol Genet* 2019;29(11):1757–1771.
42. Hukema RK, Buijsen RA, Raske C, Severijnen LA, Nieuwenhuizen-Bakker I, Minneboo M, et al. Induced expression of expanded CGG RNA causes mitochondrial dysfunction in vivo. *Cell Cycle* 2014;13(16):2600–2608.
43. Chapple JP, Bros-Facer V, Butler R, Gallo JM. Focal distortion of the nuclear envelope by huntingtin aggregates revealed by lamin immunostaining. *Neurosci Lett* 2008;447(2–3):172–174.
44. Sellier C, Buijsen RAM, He F, Natla S, Jung L, Tropel P, et al. Translation of expanded CGG repeats into FMRpolyG is pathogenic and may contribute to fragile X tremor ataxia syndrome. *Neuron* 2017;93(2):331–347.
45. Friedrich J, Kordasiewicz HB, O'Callaghan B, Handler HP, Wagener C, Duvick L, et al. Antisense oligonucleotide-mediated ataxin-1 reduction prolongs survival in SCA1 mice and reveals disease-associated transcriptome profiles. *JCI Insight* 2018;3(21):e123193.
46. Aizenman CD, Linden DJ. Regulation of the rebound depolarization and spontaneous firing patterns of deep nuclear neurons in slices of rat cerebellum. *J Neurophysiol* 1999;82(4):1697–1709.
47. Raman IM, Bean BP. Ionic currents underlying spontaneous action potentials in isolated cerebellar Purkinje neurons. *J Neurosci* 1999;19(5):1663–1674.
48. Wolfart J, Neuhoff H, Franz O, Roeper J. Differential expression of the small-conductance, calcium-activated potassium channel SK3 is critical for pacemaker control in dopaminergic midbrain neurons. *J Neurosci* 2001;21(10):3443–3456.
49. Nelson AB, Krispel CM, Sekirnjak C, du Lac S. Long-lasting increases in intrinsic excitability triggered by inhibition. *Neuron* 2003;40(3):609–620.
50. Le Bon-Jego M, Yuste R. Persistently active, pacemaker-like neurons in neocortex. *Front Neurosci* 2007;1(1):123–129.
51. Ebner BA, Ingram MA, Barnes JA, Duvick LA, Frisch JL, Clark HB, et al. Purkinje cell ataxin-1 modulates climbing fiber synaptic input in developing and adult mouse cerebellum. *J Neurosci* 2013;33(13):5806–5820.
52. Hatanaka Y, Watase K, Wada K, Nagai Y. Abnormalities in synaptic dynamics during development in a mouse model of spinocerebellar ataxia type 1. *Sci Rep* 2015;5:16102.
53. Uhlhaas PJ, Singer W. Neural synchrony in brain disorders: relevance for cognitive dysfunctions and pathophysiology. *Neuron* 2006;52(1):155–168.
54. Frega M, Linda K, Keller JM, Gumus-Akay G, Mossink B, van Rhijn JR, et al. Neuronal network dysfunction in a model for Kleefstra syndrome mediated by enhanced NMDAR signaling. *Nat Commun* 2019;10(1):4928.
55. Hurez R, Servais L, Orduz D, Gall D, Millard I, de Kerchove d'E A, et al. Aminopyridines correct early dysfunction and delay neurodegeneration in a mouse model of spinocerebellar ataxia type 1. *J Neurosci* 2011;31(33):11795–11807.
56. Duvick L, Barnes J, Ebner B, Agrawal S, Andresen M, Lim J, et al. SCA1-like disease in mice expressing wild-type ataxin-1 with a serine to aspartic acid replacement at residue 776. *Neuron* 2010;67(6):929–935.
57. Shakkottai VG, do Carmo Costa M, Dell'Orco JM, Sankaranarayanan A, Wulff H, Paulson HL. Early changes in cerebellar physiology accompany motor dysfunction in the polyglutamine disease spinocerebellar ataxia type 3. *J Neurosci* 2011;31(36):13002–13014.
58. Chopra R, Shakkottai VG. Translating cerebellar Purkinje neuron physiology to progress in dominantly inherited ataxia. *Future Neurol* 2014;9(2):187–196.
59. Dell'Orco JM, Wasserman AH, Chopra R, Ingram MA, Hu YS, Singh V, et al. Neuronal atrophy early in degenerative ataxia is a compensatory mechanism to regulate membrane excitability. *J Neurosci* 2015;35(s32):11292–11307.
60. Vagiona AC, Andrade-Navarro MA, Psomopoulos F, Petrakis S. Dynamics of a protein interaction network associated to the aggregation of polyQ-expanded ataxin-1. *Genes* 2020;11(10):1129.
61. Dissanayake K, Toth R, Blakey J, Olsson O, Campbell DG, Prescott AR, et al. ERK/p90(RSK)/14-3-3 signalling has an impact on expression of PEA3 Ets transcription factors via the transcriptional repressor capicua. *Biochem J* 2011;433(3):515–525.
62. Ahmad ST, Rogers AD, Chen MJ, Dixit R, Adnani L, Frankiw LS, et al. Capicua regulates neural stem cell proliferation and lineage specification through control of Ets factors. *Nat Commun* 2019;10(1):2000.
63. Weissmann S, Cloos PA, Sidoli S, Jensen ON, Pollard S, Helin K. The tumor suppressor CIC directly regulates MAPK pathway genes via histone deacetylation. *Cancer Res* 2018;78(15):4114–4125.
64. Wang B, Krall EB, Aguirre AJ, Kim M, Widlund HR, Doshi MB, et al. ATXN1L, CIC, and ETS transcription factors modulate sensitivity to MAPK pathway inhibition. *Cell Rep* 2017;18(6):1543–1557.
65. Shimobayashi E, Kapfhammer JP. Calcium signaling, PKC gamma, IP3R1 and CAR8 link spinocerebellar Ataxias and Purkinje cell dendritic development. *Curr Neuropharmacol* 2018;16(2):151–159.

Supporting Data

Additional Supporting Information may be found in the online version of this article at the publisher's web-site.